NREL/TP-451-5652 • UC Category: 273 • DE93018201

Polycrystalline Thin-Film Cadmium Telluride Solar Cells Fabricated by Electrodeposition

Annual Subcontract Report 20 March 1992 – 19 March 1993

J. U. Trefny, T. E. Furtak, N. Wada,
D. L. Williamson, D. Kim
Colorado School of Mines
Golden, Colorado

NREL technical monitor: B. von Roedern

National Renewable Energy Laboratory
1617 Cole Boulevard
Golden, Colorado 80401-3393
Operated by Midwest Research Institute
for the U.S. Department of Energy
under Contract No. DE-AC02-83CH10093

Prepared under Subcontract No. XG-2-11036-4

August 1993

NOTICE

Printed in the United States of America
Available from:
National Technical Information Service
U.S. Department of Commerce
5285 Port Royal Road
Springfield, VA 22161

Price: Microfiche A01
Printed Copy A03

Codes are used for pricing all publications. The code is determined by the number of pages in the publication. Information pertaining to the pricing codes can be found in the current issue of the following publications which are generally available in most libraries: *Energy Research Abstracts (ERA)*; *Government Reports Announcements and Index (GRA and I)*; *Scientific and Technical Abstract Reports (STAR)*; and publication NTIS-PR-360 available from NTIS at the above address.

Printed on recycled paper

Executive Summary

This report contains results from the first year of a three-year program at Colorado School of Mines entitled "Polycrystalline Thin Film Cadmium Telluride Solar Cells Fabricated by Electrodeposition". As described in Section 4, the work is based upon earlier studies performed by Ametek Corporation. In addition to establishment of the laboratory itself, the first year's activities included development work on each of the specific layers of the Ametek n-i-p structure as well as additional studies of several transparent conducting oxides.

Section 6 of this report describes the principal results of our work. In the case of the transparent conducting oxides, thin films of ZnO and of ZnO:Al were deposited under various conditions in close collaboration with scientists at NREL. Studies of the electrical and optical properties were reported in November, 1992. For the n-layer of the Ametek structure, a dip coating method was developed for the deposition of CdS films, again in close collaboration with NREL. Data on the characterization of these films by x-ray diffraction, Raman spectroscopy, scanning tunneling microscopy, small-angle x-ray scattering, and other techniques are reported here.

A major portion of our efforts has been directed toward the electrodeposition of the CdTe i-layer of the Ametek structure. This report describes our progress in developing appropriate electrochemical baths and in understanding the role of the many experimental parameters which must be controlled in order to obtain high-quality films of this material. Several post-deposition steps are also described including heat treatments, etching procedures, and a photoresist technique for filling pinholes in the films. X-ray diffraction data are presented to show that the Ametek process for this step has essentially been reproduced, although some additional improvments in film quality must still be achieved.

We have explored the possiblity of using an electrochemical process for fabricating the ZnTe p-layer. Some preliminary success has been achieved as shown by x-ray diffraction data. We plan to pursue this step vigorously in the next phase of the project.

Finally, we have fabricated a number of photovoltaic "dot" cells in the structure glass/SnO_2/CdS/CdTe/Au. Several cells with efficiencies in the range of 5-6% were obtained in August 1992. However, at that time we began a systematic, in-depth study of the electrochemical process for the CdTe layer. Since then, using a succession of baths, we have made steady progress toward improved and reproducible cell efficiencies in the above geometry. We are confident, given this recent progress, that cells with efficiencies in excess of 10% will be achieved in the near future.

3. Table of Contents

1.	Title Page		1
2.	Executive Summary		3
3.	Table of Contents		4
	a)	List of Figures	5
4.	Background		6
5.	Phase I Tasks and Milestones		7
6.	Accomplishments		9
	a)	Transparent Conducting Oxide Studies	9
	b)	CdS	11
	c)	CdTe	22
	d)	ZnTe	27
	e)	Devices	30
	f)	Analytical Facilities	33
7.	Summary and Plans		34
8.	References		37
9.	Appendices		39
	a)	Personnel	39
	b)	Laboratory Improvements	40
	c)	Publications	41

List of Figures

1. X-ray diffraction data for dip-coated CdS film deposited on SnO_2-coated glass.
2. X-ray diffraction data for dip-coated CdS film deposited on bare glass.
3. Raman scattering data for annealed, dip-coated CdS films on bare glass and on SnO_2-coated glass.
4. Comparison of XRD traces for samples of Figure 3.
5. STM data for dip-coated CdS films on SnO_2-coated glass.
6. STM data for dip-coated CdS films on bare glass.
7. Small-angle x-ray scattering data for an as-deposited CdS film on ZnO-coated crystalline silicon. The parameter $h = 4\pi \sin \Theta/\lambda$, where 2Θ is the scattering angle and λ is the x-ray wavelength (0.15 nm).
8. Etch depths at different etch times for 0.1% Br-MeOH solution. The linear relationship indicates that the etching is a surface reaction-limited process.
9. Variation of cell efficiencies and series resistances with different etch times in 0.1% Br-MeOH solution. Both efficiency and resistance show a large difference at shorter etch times whereas the difference becomes smaller as etch time increases. Ametek's CdTe samples were used for this experiment. Cell structure is glass/SnO_2/CdS/CdTe/Au and the size is 0.03cm^2.
10. X-ray diffraction data for a CdTe film deposited onto CdS-coated, SnO_2-coated glass at CSM.
11. Comparison of XRD data for CdTe films made by Ametek and by CSM.
12. XRD data for electrochemically deposited ZnTe film.
13. Recent CSM dot-cell efficiencies versus time. The cell structure is glass/SnO_2/CdS/CdTe/Au and the size is 0.03 cm^2.

4. Background

As described in the Solicitation (LOI NO. RM-1-11036) which led to this contract, polycrystalline thin-film CdTe photovoltaics are considered among "the leading thin-film materials in terms of efficiency and long-term reliability". Prominent companies in the development of this technology have included Photon Energy and Ametek in the U.S., Matsushita in Japan, and British Petroleum in the U.K. In 1990, Ametek made a decision to abandon further development of CdTe photovoltaics and to donate all related assets (patents, laboratory know-how, and equipment) to the Colorado School of Mines Foundation. The Ametek facility was re-established at the Physics Department of the Colorado School of Mines and formed the basis, along with the laboratory know-how, for the current work.

The Ametek research, supported to a large extent by NREL (SERI), led to small cells of more than 11% efficiency. Moreover, the unique, low cost electrodeposition methods developed by Ametek for this material have attracted a great deal of interest. At the same time, additional basic research is still needed to improve upon the efficiencies and performance levels achieved to date. Among the significant issues are interface carrier recombination and top-layer photon absorption which presently limit the short-circuit current, junction recombination which limits the open-circuit voltage, and series-resistance losses which suppress the fill-factor. Cascade geometries based on CdTe-containing ternaries are also an area of interest. With respect to large-scale processing and manufacture, some of the pressing issues are the design of suitable equipment, efficient methods for making interconnections on large arrays, and suitable packaging.

The intent of the CSM contract is to build upon the Ametek experience and expertise regarding polycrystalline, thin-film, CdTe n-i-p solar cells to improve certain processing steps and the potential for economic, large-scale production. Improved efficiencies are also a major goal. Significant increases should be possible through interface and grain-boundary passivation, antireflection coatings, and other improvements. High-quality film growth techniques, materials analysis, device characterization, and device fabrication are all of particular interest in our work.

The Ametek n-i-p structure contains at least 3 different semiconducting layers, comprised of at least 4 different elements, as well as front and back ohmic contacts. The preferred embodiment involves a common anion at the p-i junction and a common cation at the i-n junction [1]. Intermediate layers are possible, which might be introduced to passivate defects or act as buffer layers since interdiffusion of materials at the boundaries can be problematic.

A variety of deposition procedures has previously been used for the respective layers. Although a spray pyrolysis technique for the CdS n-layer was developed and patented by Ametek, their highest efficiency cell was achieved with a dip coat method for this part of the structure. Their approach involved the use of $CdCl_2$, NH_4OH, NH_4Cl and thiourea at about 100°C.

An important part of the Ametek technology is the CdTe i-layer electrodeposition process which leads to insulating, compensated CdTe, an essential feature of the overall structure. There are trap states at one of the CdTe band edges which have been identified, in bulk samples, by DLTS

and photoluminescence [2]. Their origin is thought to be Cd vacancies. However, other possibilities include grain boundaries and the internal surfaces of microvoids.

The Ametek technique for the fabrication of the ZnTe p-layer was vacuum thermal deposition. As part of the development of a more practical overall process, our project includes the investigation of non-vacuum methods for this step. To complete the process, non-vacuum methods for metallization would also be desirable.

5. Phase I Tasks and Milestones

The Phase-One film-growth activities were intended to involve all three layers of the n-i-p cell structure. For the CdS layer, dip coating, electroplating, and the sequential formation of CdS by plating and subsequent chemical reaction were to be tested and evaluated as substitutes for spray pyrolysis. A goal was to establish one of these approaches, or an alternative to be identified, as most favorable before the end of the first year of the project. For the CdTe layer, we planned to continue to use an electrodeposition process, but studies to improve the final product by photoelectrochemical stimulation were also intended to be carried out. The Phase-One goal of this aspect of the project was to establish whether the i-layer can be improved with respect to grain size and/or grain boundary passivation by this photoelectrochemical approach. With respect to the ZnTe layer, an effort was to be made in Phase One to discover an alternative to vacuum deposition. The goal of the first year of the program in this instance was to demonstrate at least one viable alternative such as electroplating. For all three layers, we were to explore the use of rapid thermal processing in the first year in collaboration with existing expertise at NREL.

The second task, device fabrication, was also to begin immediately in Phase-One. The goal during the first twelve months was to establish a CSM capability for the fabrication of small-scale cells comparable to those produced earlier at Ametek. These devices are needed to serve as baseline standards against which new devices made by alternative or improved processing steps as described above can be compared.

The remaining tasks were materials analysis and device characterization. In the first year, our goal was to develop and refine the standard testing capabilities at CSM to the point that the evaluation of both single layers and entire devices becomes routine.

A Table of specific Phase One tasks is given on the following page.

Phase One Tasks

Task one (high quality film growth techniques):

1. establish dip coating, electroplating, sequential formation, or some other process as an alternative to spray pyrolysis for the deposition of CdS
2. establish the effects of photoenhancement on the electrochemical deposition of CdTe with respect to grain size, grain boundary passivation, and other characteristics of the product
3. demonstrate an alternative to the vacuum deposition of ZnTe
4. begin experiments with rapid thermal processing

Task two (device fabrication):

1. manufacture 1 cm^2 CdTe cells having an efficiency of at least 10%

Task three (materials analysis):

1. set up and test facilities for the routine analysis of materials by resistivity, optical transmission, XRD, Raman spectroscopy, SAXS, etc.

Task four (device characterizations):

1. set up and test facilities for the measurement of I-V curves, C-V characteristics and cell efficiencies

6. Accomplishments

a) Transparent Conducting Oxide Studies

Although the work is not directly related to the Ametek CdTe cell structure, one of the tasks of this contract was to investigate the properties of ZnO films deposited by ion-sputtering techniques. This effort was undertaken by a graduate student, Mr. Yi Qu, who worked in close collaboration with scientists at NREL.

The structural, electrical and optical properties of undoped and Al-doped ZnO films were studied under this task. XRD and STM measurements revealed that the grain size both perpendicular and parallel to the substrate increases with film thickness and deposition temperature. The largest size perpendicular to the substrate was found to be ~100 nm. In addition, the grain size in the direction perpendicular to the substrate is nearly proportional to film thickness up to a thickness of 1,150 nm as investigated in this study and, furthermore, it is dependent upon the deposition temperature. In particular, the grain size saturates when the deposition temperature is higher than 250°C. Thereafter, the grain size perpendicular to the substrate, in another words the film thickness, becomes more critical to the transport properties. This observation is consistent with the experimental results for the electrical properties. For a fixed film thickness for deposition temperatures exceeding 250°C, the resistivity does not change much with deposition temperature, but it still remains sensitive to film thickness.

The electrical resistivity of undoped ZnO thin films was determined using both Hall measurements and a 4-point probe. Undoped ZnO films have a wide range of resistivity from ~10^{-3}-10^{7} Ω-cm depending on deposition parameters and film thickness. Hall measurements were carried out for films with resistivity lower than 10^{2} Ω-cm. For films with resistivity higher than 10^{2} Ω-cm, Hall measurements could not be made because of the difficulty involved in forcing a current through such resistive layers. For these films the resistivity was obtained through the relation $\rho = R_s t$, where R_s is the sheet resistance measured using a 4-point probe and t is the film thickness. Films with a low resistivity of 10^{-3}-10^{-2} Ω-cm were deposited in a mixture of Ar and H_2. In this case, the carrier concentration of as-deposited films could be as high as 10^{20} cm^{-3}, this being the main reason for the low resistivity. However, the resistivity is not stable in this case, increasing with the exposure time (over a period of days) in air. Films with a high resistivity of more than 10^{2} Ωcm were deposited in a mixture of Ar and 0_2. Because it was not possible to do Hall measurements on these films, information about carrier concentrations and mobilities is not available. Films with medium resistivity from 10^{-1}-10^{2} Ω-cm were deposited in pure Ar. These films have a carrier concentration of 10^{17}-10^{19} cm^{-3} and mobility of 1-25 cm^2/V-s depending on film thickness and deposition temperature.

Undoped ZnO films were deposited in a mixture of H_2 and Ar to study the effect of H_2 on electrical properties. The results showed that the resistivity decreases dramatically when a small amount of H_2 is introduced into the deposition chamber. Subsequently, it decreases more slowly and eventually levels off when more H_2 is added. Carrier concentration and mobility results show that the rapid decrease of resistivity is due to both an increase in carrier concentration and mobility. However, the resistivity is not stable as mentioned earlier. When these films are exposed in air, even

at room temperature, the resistivity increases. After about three weeks, the resistivity reaches values comparable to those of films deposited in pure Ar.

Electrical and optical properties of as-deposited, ion-beam-sputtered ZnO:Al films were studied as a function of film thickness and carrier concentration. Hall measurements revealed a general decrease in the bulk electrical resistivity with increasing film thickness. For thinner films, the resistivity decreased rapidly with film thickness. In this regime, with an increase in film thickness from 100 to 200 nm, a significant decrease in resistivity from 2.8×10^{-2} to 4.4×10^{-3} Ω-cm was attributed to increases in both carrier concentration and Hall mobility. For thicker films, the resistivity was relatively insensitive to film thickness and approached a value of ~8.6×10^{-4} Ω-cm at a thickness of 1,100 nm. In this thickness regime, the slight decrease in resistivity with increasing film thickness was attributed to an increase in carrier concentration alone. The above observations suggest the presence of at least two scattering mechanisms. It is speculated that grain boundary scattering and ionized impurity scattering are most likely. These issues, together with the observed optical properties of the films, were discussed in a presentation at the American Vacuum Society National Symposium in November, 1992[3].

b) CdS Processing and Characterization

CdS is an important II-VI semiconductor which can be used to make n-type window-layers for polycrystalline photovoltaic applications. The subject of active research over the past three decades, CdS thin films can be made by different techniques such as vapor deposition, sputtering, electroplating, chemical spray deposition, and chemical bath deposition.

Chemical bath deposition (CBD), sometimes referred to as solution growth or dip coating, is a very attractive method to produce CdS thin films for polycrystalline solar cells such as CdTe and $CuInSe_2$. Using CdS grown by CBD, the highest efficiencies of CdTe cells are currently about 15.2% and of $CuInSe_2$ cells about 14.2%, produced by groups at the University of South Florida and at Stuttgart University, respectively. Chemical bath deposition is a simple, inexpensive and reproducible method for large area deposition at low temperatures.

The chemical bath deposition of CdS thin films is made from cadmium salts ($CdSO_4$, $CdAc_2$, $CdCl_2$, etc), an organic sulfur-containing reducing agent (Thiourea, NH_2CSNH_2 or thioacetamide, NH_2CSCH_3), and ammonia. There are two growth models in the formation of CdS thin films by chemical bath deposition[4]. One is the ion-by-ion model in which the growth of the film takes place by condensation of Cd^{+2} and S^{-2} ions. This model results in thin, hard, and adherent films. Another is the cluster-by-cluster model in which the growth of the film takes place by adsorption of colloidal particles of CdS which are formed in the solution. This model results in thick, and powdery films.

It is well known that the deposition of CdS occurs when the ionic product of $[Cd^{+2}]$ and $[S^{-2}]$ exceeds the solubility product (K_{sp}) of CdS. Even though the solubility product of CdS is very low (about 1.4×10^{-29}), the precipitation of CdS can take place easily. In order to avoid a lot of precipitation, the preparation of CdS thin films should be based on the slow release of Cd^{+2} and S^{-2} in solution. The ionic product of Cd^{+2} and S^{-2} is desired to just barely exceed the solubility product of CdS. In this case, the nucleation and growth of CdS films will be by ion-by-ion condensation. Slow release of the Cd^{+2} ions can be achieved by the dissociation of a complex species of cadmium. The S^{-2} ions can be prepared by decomposition of thiourea in alkaline solution.

A reaction mechanism for the formation of CdS is suggested below[5,6]:

(a) Ammonium hydroxide in an aqueous solution to form an alkaline solution and a complexing agent:

$$NH_3 + H_2O \leftrightarrow NH_4^+ + OH^- \quad (1)$$

(b) Cadmium salts in an ammonium hydroxide solution to form the complex compounds:

$$CdSO_4 + 4(NH_3) \leftrightarrow (Cd(NH_3)_4)SO_4 \quad (2)$$

$$Cd(NH_3)_4^{+2} \leftrightarrow Cd^{+2} + 4NH_3 \quad (3)$$

$$Cd(OH)_2 \leftrightarrow Cd^{+2} + 2(OH)^- \quad (4)$$

$$Cd(OH)_2 + 2(NH_3) \leftrightarrow Cd(NH_3)_2^{+2} + 2(OH)^- \quad (5)$$

(c) In the case of thiourea as the sulfide-ion source in an alkaline medium, the sulfide ions are released as follows:

$$(NH_2)_2CS + 3OH^- \leftrightarrow 2NH_3 + CO^{-2} + SH^- \quad (6)$$

$$SH^- + OH^- \leftrightarrow S^{-2} + H_2O \quad (7)$$

(d) Cadmium ions react with sulfide ions to form CdS from equations (3), (4), and (7):

$$Cd^{+2} + S^{-2} \leftrightarrow CdS \quad (8)$$

The reactions shown in Equations 1 to 8 are interrelated. The ammonia concentration affects the concentration of cadmium ions, the precipitation of cadmium hydroxide, the concentration of the tetraammine-cadmium complex ion, and the concentration of hydroxide ions. The hydroxide ion concentration also affects the decomposition of thiourea, the formation of cadmium hydroxide, and the concentration of complex ions.

When the ionic product of the concentrations of cadmium cation and sulfide anion exceeds the solubility product K_{sp} of CdS, a CdS thin film should be deposited heterogeneously from the preferential adsorption of Cd^{+2} or S^{-2} ions followed by the addition of S^{-2} or Cd^{+2} ions on the substrate surface. At the same time, CdS will precipitate homogeneously in solution.

One reaction mixture was prepared from $CdAc_2$(10^{-3}M), NH_4Ac (0.02M), NH_4OH (0.4M), and $(NH_2)_2CS$ (5 x 10^{-3}M) in an aqueous solution[7]. With a pH value of about 9, the mixture was warmed up from room temperature to about 82°C under constant stirring. The nucleation of CdS started after about 10 min. CdS thin films were then deposited on SnO_2-coated glass substrates at a rate of about 1000Å in 50 min. The average deposition rate was about 25Å/min with a concentration ratio of [$CdAc_2$] to [$(NH_2)_2CS$] of about 1/5.

Another reaction mixture was prepared from $CdSO_4$ (1.5 x 10^{-3}M), NH_4OH (1.8M), and $(NH_2)_2CS$ (1.5 x 10^{-1}M) or $(NH_2)_2CS$ (1.5 x 10^{-2}M) in an aqueous solution. With a pH value of about 11, and a warm-up from room temperature to about 82°C under constant stirring, the nucleation of CdS started after about 2.5 min for $(NH_2)_2CS$ (1.5 x 10^{-1}M) or after about 3.0 min for $(NH_2)_2CS$ (1.5 x 10^{-2}M). CdS thin films were deposited on SnO_2-coated glass substrates at a rate of about 1000Å in 20 min. The average deposition rate was about 50Å/min at a concentration ratio of [$CdSO_4$] to [$(NH_2)_2CS$] between 0.01 and 0.1. Using these techniques, CdS thin films can be deposited on various substrates such as SnO_2-coated glass, ZnO-coated glass, crystalline Si, 7059-glass, and CIS.

Our characterization studies of CdS have included electrical resistivity measurements, x-ray diffraction measurements (XRD), scanning-tunneling-microscope imaging (STM), Raman scattering, and small-angle x-ray scattering (SAXS). Sheet resistivities are typically in the range of

2 to 15 Ω/□. A systematic correlation of resistivity data with deposition and annealing conditions is currently underway.

Figures 1 and 2 show XRD traces from samples MG27 and MG28 to document the formation of CdS by the method of Chu as developed by Mr. Du. Similar XRD results are obtained for both bare glass and SnO_2-coated glass: (1) the as-deposited CdS consists of a small grain-size hexagonal (h) or cubic (c) structure with a strong preferred orientation of the (002) [h] or (111) [c] grains parallel to the film surface; (2) the annealed CdS is clearly the hexagonal structure with a near-random grain orientation. The films are typically annealed in nitrogen for 50 minutes at a temperature of 450°C after a dip coating of $CdCl_2$.

The Raman scattering technique was also used to characterize the CdS thin films. A well-crystallized, large CdS single crystal (obtained from Dr. Alan Fahrenbruch at Stanford University) exhibits an LO mode at ~301 cm^{-1}. It is known that as the crystalline size becomes smaller, the LO peak position down-shifts and its width becomes broader[8]. Raman scattering, therefore, can be a powerful tool to probe the crystalline size and the quality of thin film CdS samples.

Figure 3 shows Raman spectra taken from CdS thin films deposited on SnO_2 and 7059 glass substrates and annealed at 450°C for 50 min. The peak position from the D31-2 sample deposited on 7059 glass was lower by ~1 cm^{-1} than that of the D31-4 sample deposited on SnO_2. Also note that the Raman peak width of the D31-2 sample was broader. The results indicate that the CdS film on SnO_2 may be better crystallized or that the grain size is larger than the film on the glass substrate. This observation is consistent with the STM work described below, where much larger grain sizes were found for the CdS films on SnO_2 substrates. These same two samples were examined by XRD (Figure 4). The improved crystallinity of the CdS on SnO_2 versus bare glass is seen via the stronger intensities of the (100), (101) and (110) peaks. (There is some overlap between the CdS (002) peak and the SnO_2 (110) peak.)

It is also noted that luminescence from CdS films when irradiated with a 5145 Å laser beam appears to be correlated to the crystallinity. The amount of luminescence from annealed CdS films was found to be two-orders-of-magnitude larger than that of unannealed films. When the crystallinity is poor, the excited carriers may decay through non-radiative channels.

Recent STM measurements performed at NREL on Mr. Du's films show clearly that the morphology is significantly dependent upon the nature of the substrate. Films deposited onto bare 7059 glass show dominant features on a scale of several hundred Angstroms while those deposited under similar conditions onto tin-oxide-coated glass display dominant features approximately ten times as large. Examples of these cases are shown in Figures 5 and 6. Further studies on other substrates and after various heat-treatments are underway.

We have obtained a first set of SAXS results from a CdS film deposited on ZnO-coated c-Si. Figure 7 compares the as-deposited CdS with the ZnO/Si substrate and demonstrates a relatively strong SAXS signal due to some type of electron density fluctuation. The predominant size of the scattering centers is about 1.3 nm; if we assume they are microvoids, then a volume fraction of about

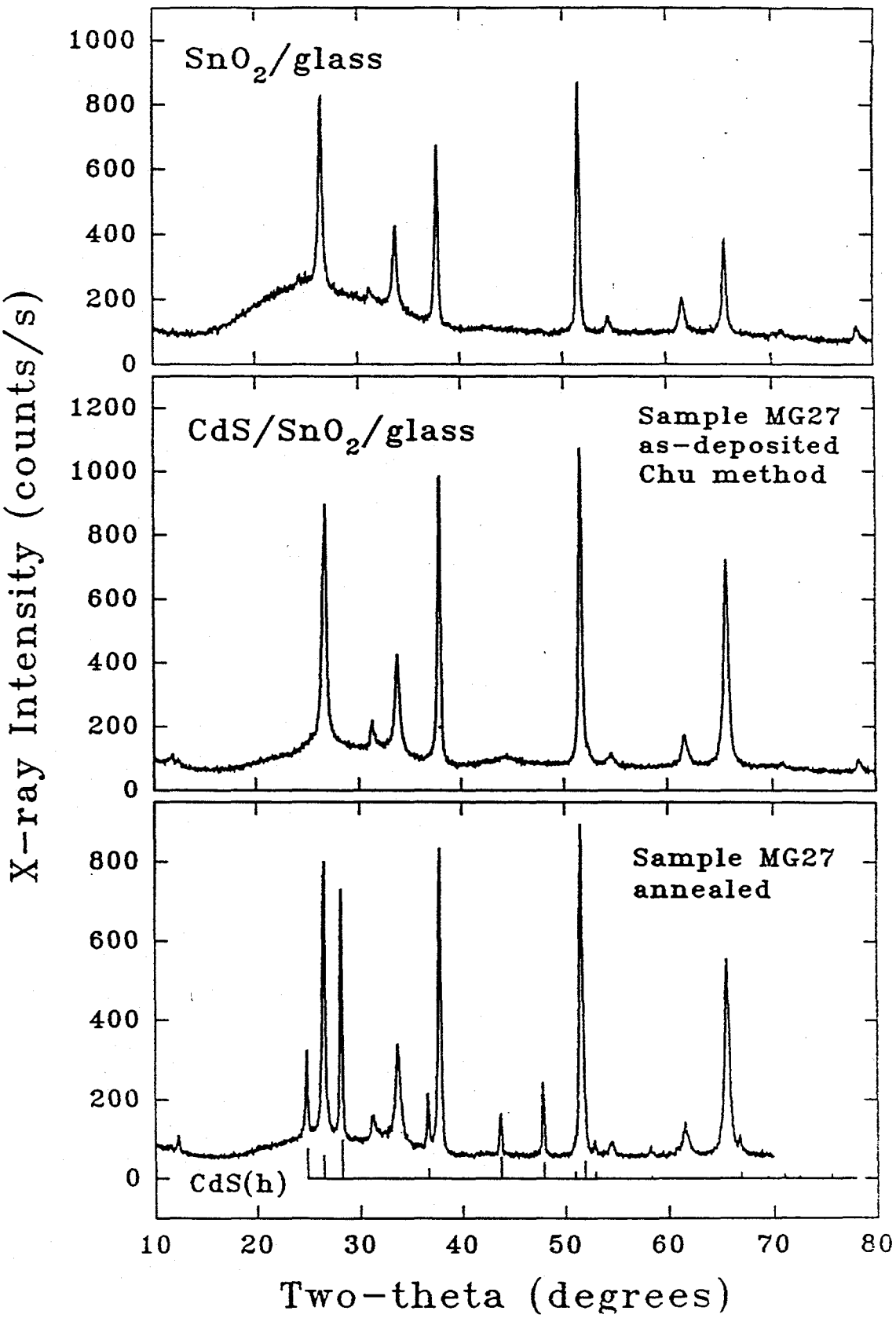

Figure 1. X-ray diffraction data for dip-coated CdS film deposited on SnO_2-coated glass.

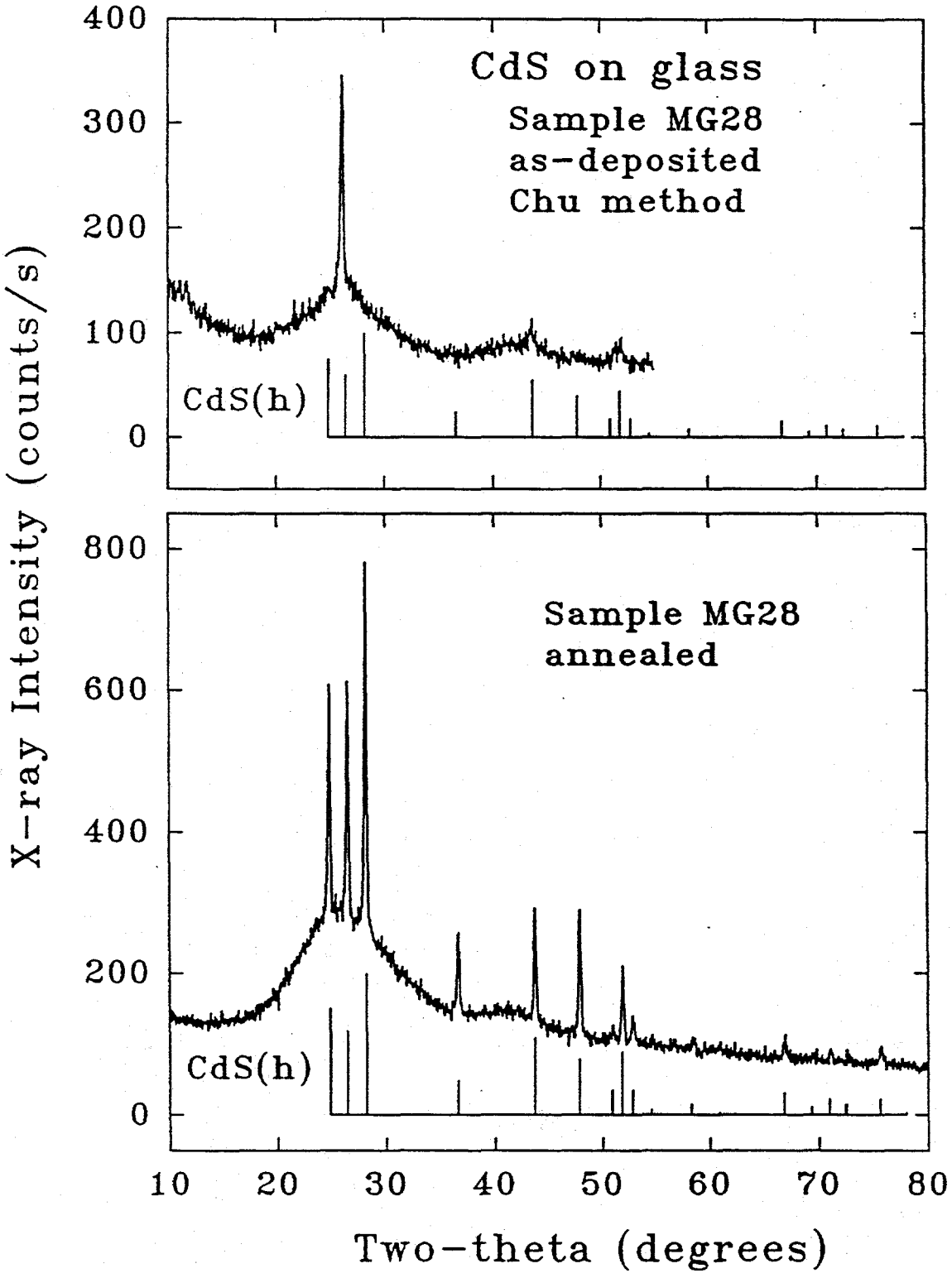

Figure 2. X-ray diffraction data for dip-coated CdS film deposited on bare glass.

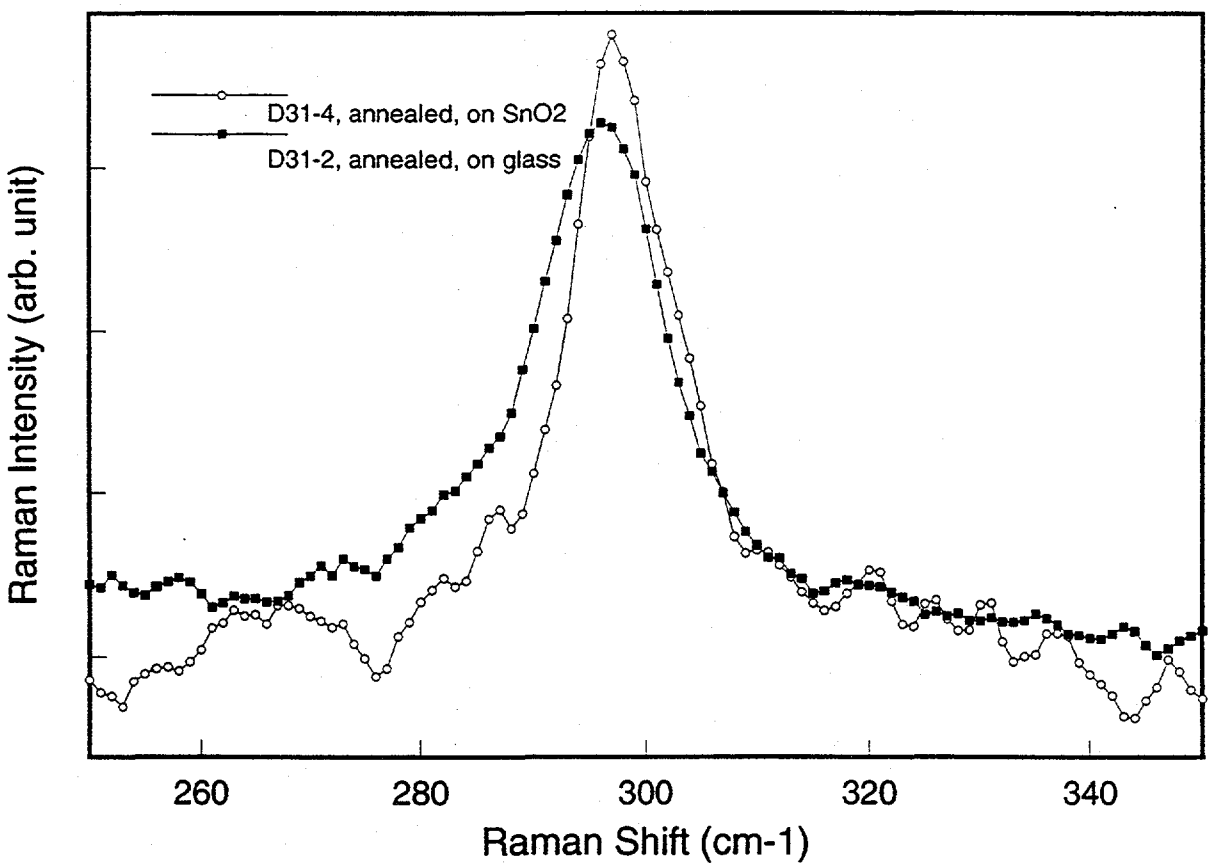

Figure 3. Raman scattering data for annealed, dip-coated CdS films on bare glass and on SnO_2-coated glass.

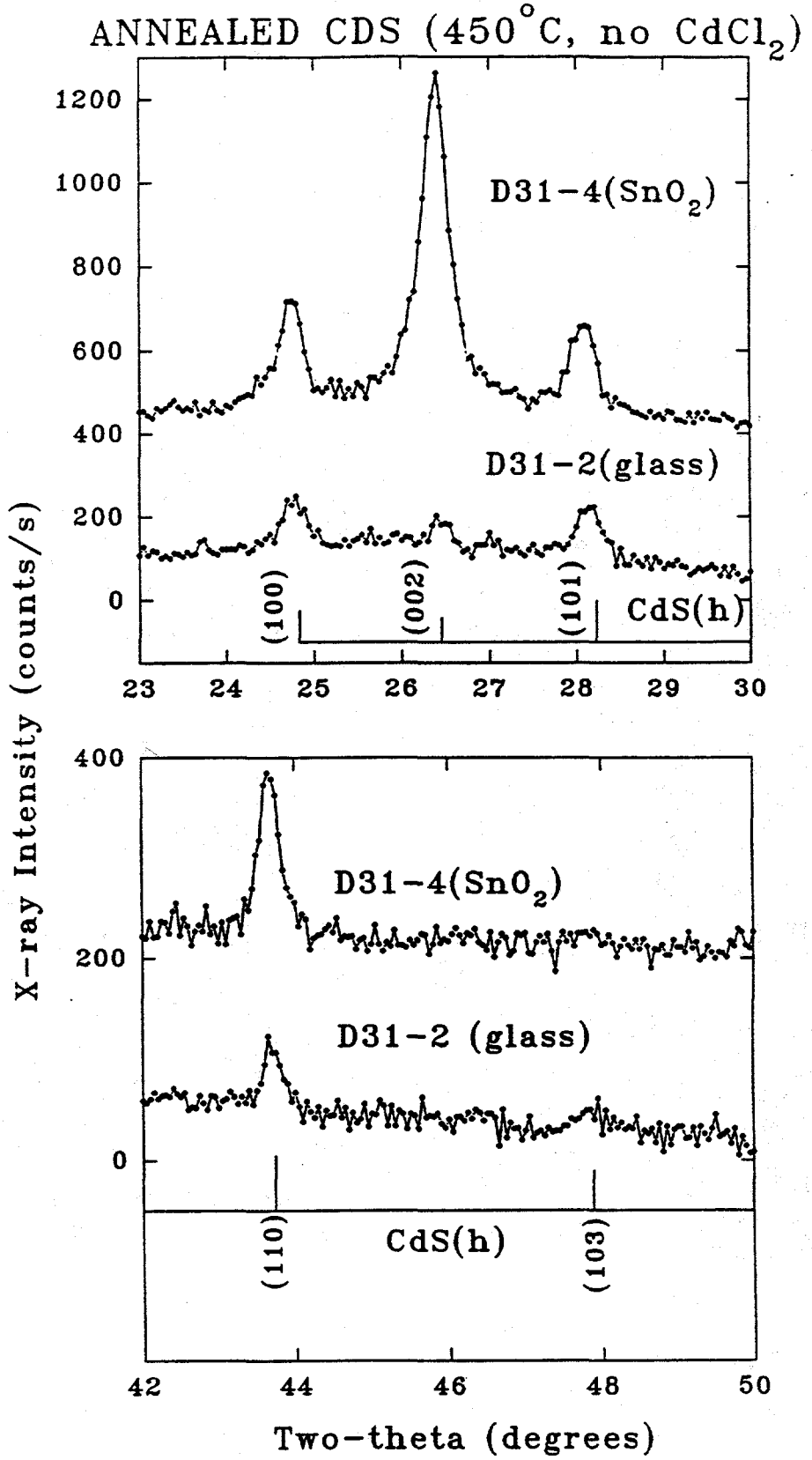

Figure 4. Comparison of XRD traces for sample for Figure 3.

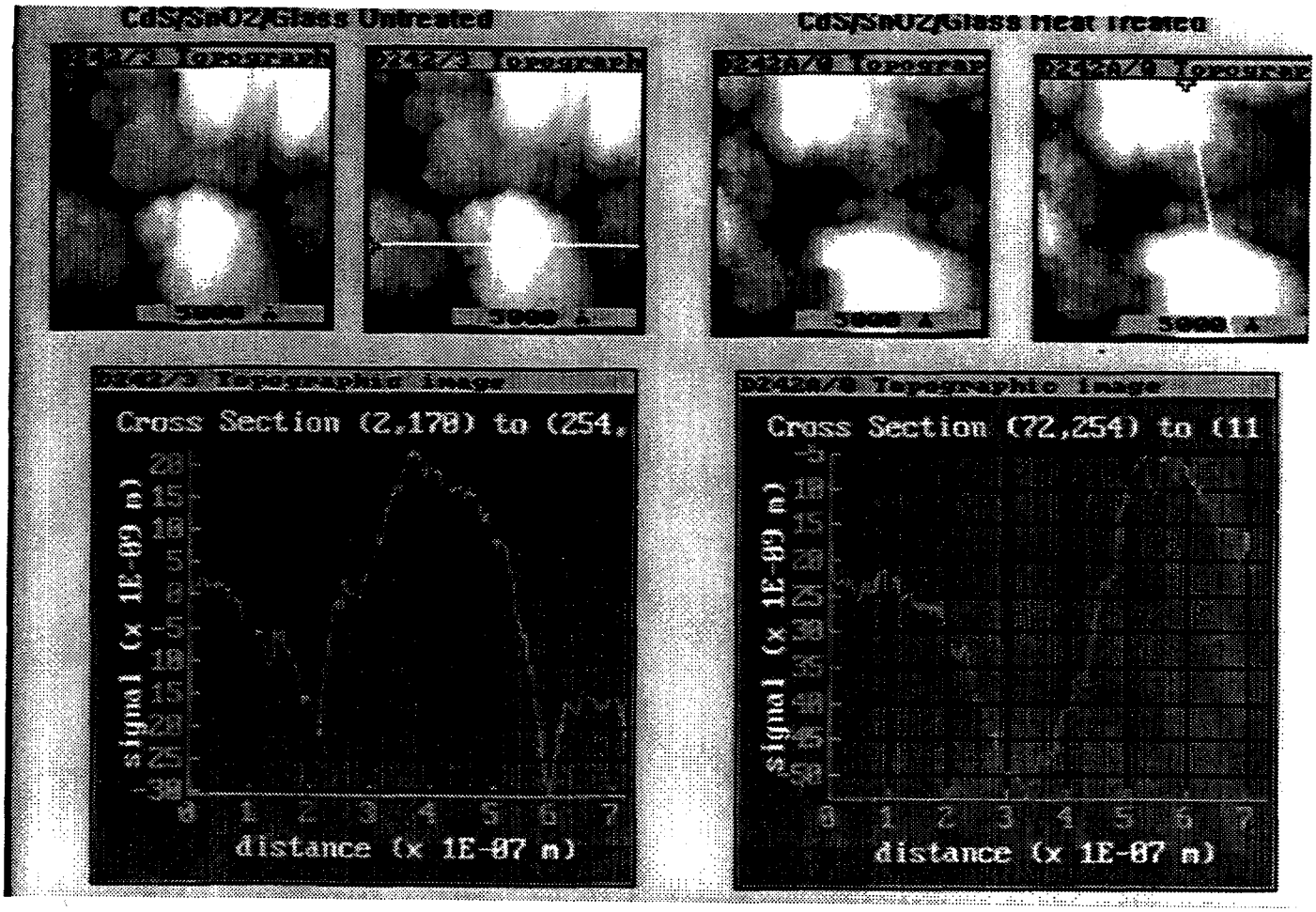

Figure 5. STM data for dip-coated CdS films on SnO_2-coated glass.

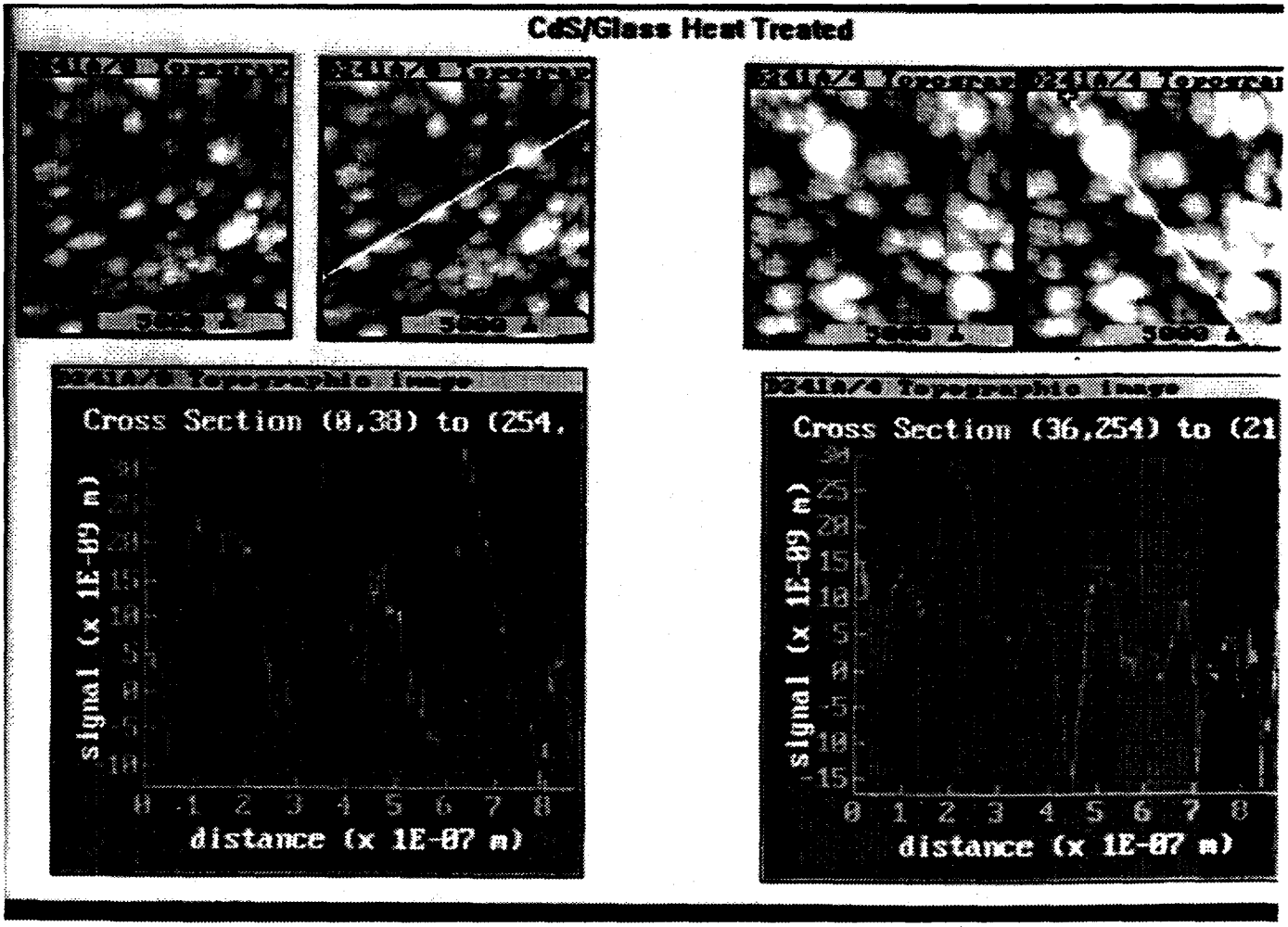

Figure 6. STM data for dip-coated CdS films on bare glass.

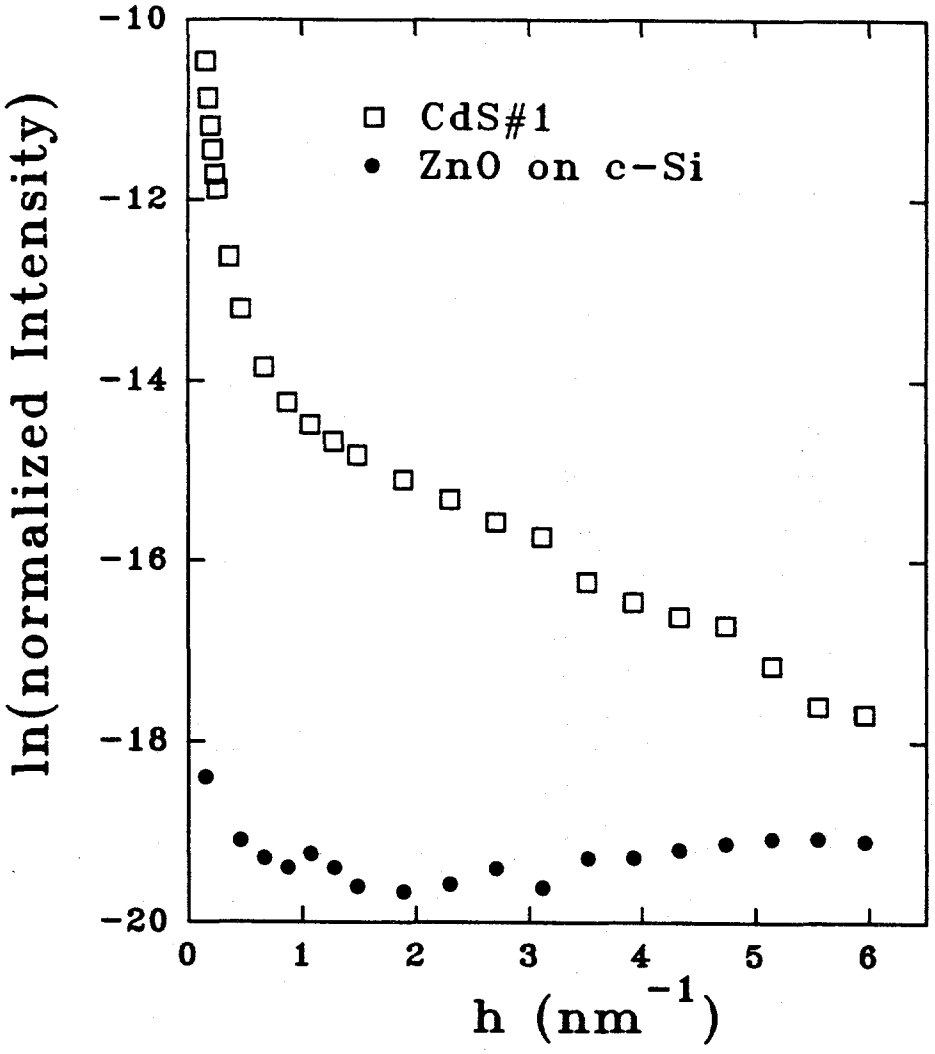

Figure 7. Small-angle x-ray scattering data for an as-deposited CdS film on ZnO-coated crystalline silicon. The parameter $h = 4\pi \sin\theta/\lambda$, where 2θ is the scattering angle and λ is the x-ray wavelength (0.15 nm).

6% is obtained. If the scatterers are some other type of defect with a density greater than zero, then an even larger volume fraction must be present since the SAXS is proportional to the electron density contrast with the CdS materials. Further experiments are underway to examine the effects of $CdCl_2$ treatment and annealing on the observed microstructure. We note that SAXS provides a means of characterizing the bulk microstructure on a scale comparable to that of the STM which characterizes the surface structure.

c) CdTe Electrochemical Deposition, Post-deposition Treatment and Characterization

i) Electrochemical Deposition

Deposition of CdTe layers with a desired microstructure - dense and uniform material with a columnar structure - is a crucial part of this project. The CdTe layers are also required to be compositionally uniform with the optimum stoichiometry since a small deviation from stoichiometry may have a significant influence on the photoelectronic properties of CdTe[9]. In order to achieve these goals, a good understanding and control of the processing parameters is necessary.

An excellent theoretical analysis of electrochemical deposition of CdTe was done by Kroger's group[10], and a good review of the theory combined with practical experimentation has been given by McDoty[11]. Different types of aqueous solutions have been studied as mediums of the deposition: sulfate solution[12], chloride solution[13], and bromide solution[14]. CdTe deposition using non-aqueous solutions has been studied by R.B. Gore et al[15].

The experimental parameters that may affect the film's properties are: the deposition current density J_{dep}, the deposition current ratio between the Te anode and the Cd anode J_{Te}/J_{Cd}, the deposition potential V_{dep}, the pH of the solution, the concentration of the Cd and Te ions in the solution [Cd] [Te], the deposition temperature T_{dep}, and the degree of agitation.

An optimization of the procedure was previously performed by a group of engineers at Ametek. However, the details of what was done and the methods that led to the use of these parameters were not very well documented. As a result, some of the crucial processing steps had to be recovered by us by reading the literature, laboratory notes and raw data scattered with other Ametek documents, and by communicating with the Ametek engineers. It is our judgement that an organized effort must still be made regarding the documentation of the Ametek work in order to save their valuable achievement from complete loss. This effort will also save us from a great deal of unnecessary experiments and trouble-shooting. Some of our research effort will be spent on this issue over the next few months.

Much of our research effort to date has been spent understanding the role of each of the experimental parameters, trouble-shooting, and trying to reproduce the Ametek results by using experimental conditions similar to those described in their reports. Our deposition system has evolved continuously from the most simple three-electrode system in a one-liter bath (a cathode, an inert anode, and a reference electrode) to a more versatile split anode system in a two-liter bath (a cathode, a Te sacrificial anode and an inert anode for Cd, and a reference electrode). The system now may run continuously with minimal loss of solution by evaporation. This system is presently

run without any filtration, which seems to be a significant disadvantage for producing high quality films.

The reason that we started to use small baths rather than the larger (30-liter) baths from Ametek is that we wanted to do experiments without being concerned about wasting the resource and creating large amounts of chemical waste because we were bound to destroy the bath often during the learning period. The knowledge and experience obtained from the small baths are now such that we are ready to begin using the large bath. The x-ray diffraction data and cell efficiencies that we are currently producing support this view.

Two processing difficulties that must still be overcome are nodular growth and Cl_2 gas generation. The cause for the nodular growth is not well understood, but it may be avoided by adopting both a continuous filtration of the solution and a dummy deposition. Our present 2-liter system does not have filtration and, as a result, the bath reaches the nodular-growth condition very quickly, typically after three runs. We have reduced the nodular-growth problem somewhat by running dummy depositions at low pH, but we have not completely removed it. We expect that the nodular growth will not be a difficulty once we switch to a larger bath with filtration. Cl_2 gas generation can be avoided by monitoring the cell voltage (between Cd/Te anodes). Chlorine gas is believed to be harmful for the microstructure of the CdTe layer and thus results in low efficiency cells.

The properties of the CdS layer may play an important role for CdTe deposition. For example, parameters such as the crystallinity, the grain size, and the surface smoothness may affect the microstructure of as-grown CdTe layers. We are now using chemically-dipped CdS either as-deposited or after annealing. It will be useful to do a comparison study to determine the effect of CdS deposited by different methods on the CdS/CdTe cell properties.

ii) Post-deposition Treatment and Characterization

As-deposited CdTe is n-type[16]. Annealing the film in air after $CdCl_2$ treatment is necessary to change the material to p-type. The $CdCl_2$ treatment is reported to enhance grain growth during the heat treatment[17] and to reduce recombination losses at the CdS/CdTe interface[18]. The sample is dipped in a 5 wt % $CdCl_2$-ethanol solution and dried in air before annealing at 410°C for 30 min in air. After being cooled in air to room temperature, the sample is etched for 30-40 sec. in 0.1% Br-MeOH solution. Au dots (0.03 cm^2) are then deposited through a mask in vacuum. The cell structure used in this work is glass/TCO/CdS/CdTe/Au. Recently we obtained a more uniform $CdCl_2$ coating by spin coating. Dip coating usually leaves streaks of white residue which is believed to contribute to non-uniform cell performance across the sample. An alternative approach is to use an ultrasonic vaporizer to make a cloud of $CdCl_2$ solution for the coating. We will compare the two techniques and apply the better one to coating the CdTe layers.

Etching the CdTe surface is necessary to remove any surface chemicals or contamination from the previous process and to remove the oxide layer, if any, at the surface. Etching is one of the important factors for making low-resistance back contacts, not only because it cleans the surface but also because it changes the surface composition (Cd/Te ratio), and thus changes the electrical

characteristics of the surface[19]. Br-MeOH solution and "Dichromate" solution are most widely used. Figure 8 shows the etch depth vs etch time relationship for a 0.1% Br-MeOH solution. The data are useful when a precise thickness control is required. As an example, CdTe samples deposited by Ametek were etched for different times and the cell efficiencies subsequently were measured. Figure 9 shows the result. The data suggest that a small variation of the thickness may have a significant effect on the cell performance.

A photoresist process has been developed and applied to fill the pinholes in the sample to reduce the problem of the shunt resistance. We have found that the photoresist treatment enhances the uniformity of cell performance across the whole film. This process will be especially useful when we start to fabricate large cells (> 1 cm^2).

Figure 10 shows X-ray diffraction data from an early CdTe film prepared at CSM (Sample CdTe#5). It was deposited on CdS which had been predeposited on SnO_2-coated glass. The top two plots show the data on a linear vertical scale while the lower plot uses a logarithmic vertical scale to display clearly the weaker peaks. To displace the data on the logarithmic plot, the annealed sample data was simply multiplied by a factor of 0.1. Identification of the phases was straightforward and, as indicated, the as-deposited film consists of cubic-CdTe, hexagonal-CdS, and SnO_2, while new peaks appeared after annealing which are similar to those from α-$CdTeO_3$ + $CdTe_2O_5$ + CdO. (There are significant disagreements in the d-spacings, however, and this may be due to non-stoichiometry in the oxides.)

The intensities of the CdTe peaks show strong preferred orientation of the grains such that the (111) planes (corresponding to strongest peak in all plots) are parallel to the film surface in the as-deposited film and a transition to a near-random texture occurs upon annealing. The decrease in intensity of the (111) peak upon annealing suggests that new grains with the other orientations grow at the expense of the (111) grains oriented parallel to the surface. The broad, weak peaks under the second and third CdTe peaks (with increasing 2θ, see log-plot) in the as-deposited film are indications of very small grains of these other orientations.

The linewidth of the CdTe (111) peak is 0.29° before and after annealing, suggesting that the crystallinity of these grains is already quite good before annealing. The XRD system yields linewidths of about 0.21° for powdered single crystalline GaAs. The other CdTe peaks have similar linewidths after annealing suggesting similar grain sizes for these other grains. XRD measurements, done in conjunction with the etching experiments described above, were used to confirm the removal of surface oxides and chloride-related phases.

Figure 11 shows XRD data from an original Ametek CdTe film (#EF344-R) in the as-deposited and annealed states, and compares it to CSM #C-43, also as-deposited and annealed. The similarity is striking and indicates that the Ametek process for CdTe is being closely duplicated at CSM. Note that the as-deposited film has a very strong preferred orientation of the (002) [h] or (111) [c] crystallites, while after annealing the CdTe is clearly the cubic phase with a near-random grain orientation. All of the peaks except those circled can be accounted for by CdTe (c), CdS(h), and SnO_2. The two peaks circled on the Ametek sample XRD pattern may be $Cd_3Cl_2O_2$, a compound left over from the anneal process.

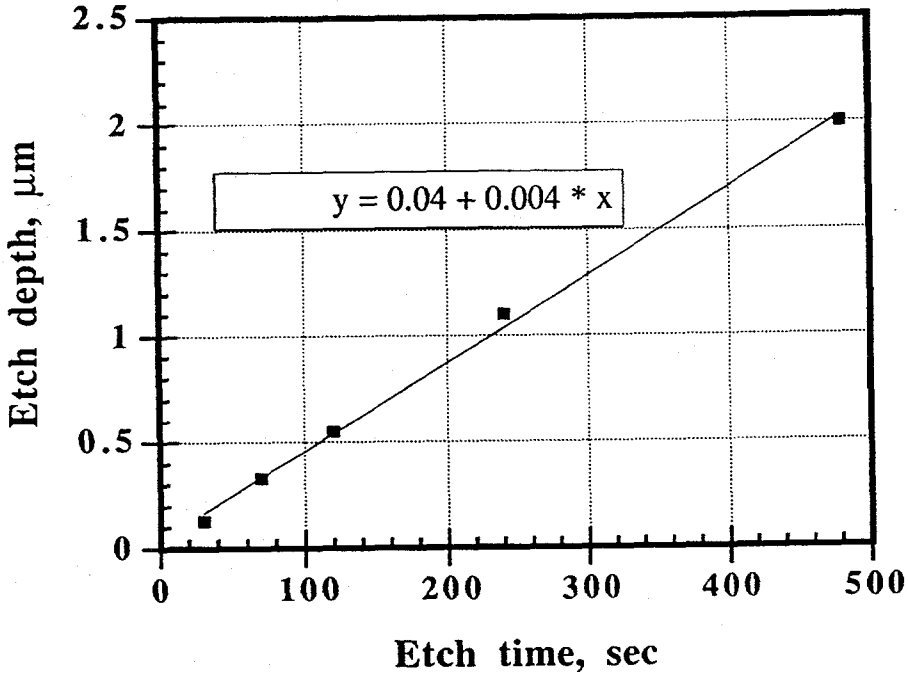

Figure 8. Etch depths at different etch times for 0.1% Br-MeOH solution. The linear relationship indicates that the etching is a surface reaction-limited process.

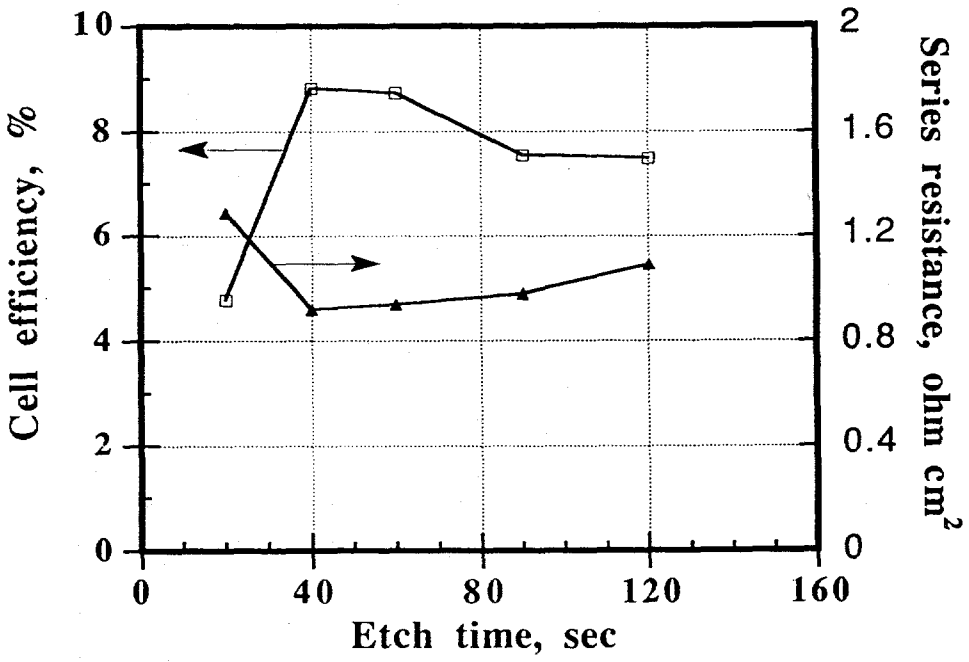

Figure 9. Variation of cell efficiencies and series resistances with different etch times in 0.1% Br-MeOH solution. Both efficiency and resistance show a large difference at shorter etch times whereas the difference becomes smaller as etch time increases. Ametek's CdTe samples were used for this experiment. Cell structure is glass/SnO_2/CdS/CdTe/Au and the size is 0.03 cm^2.

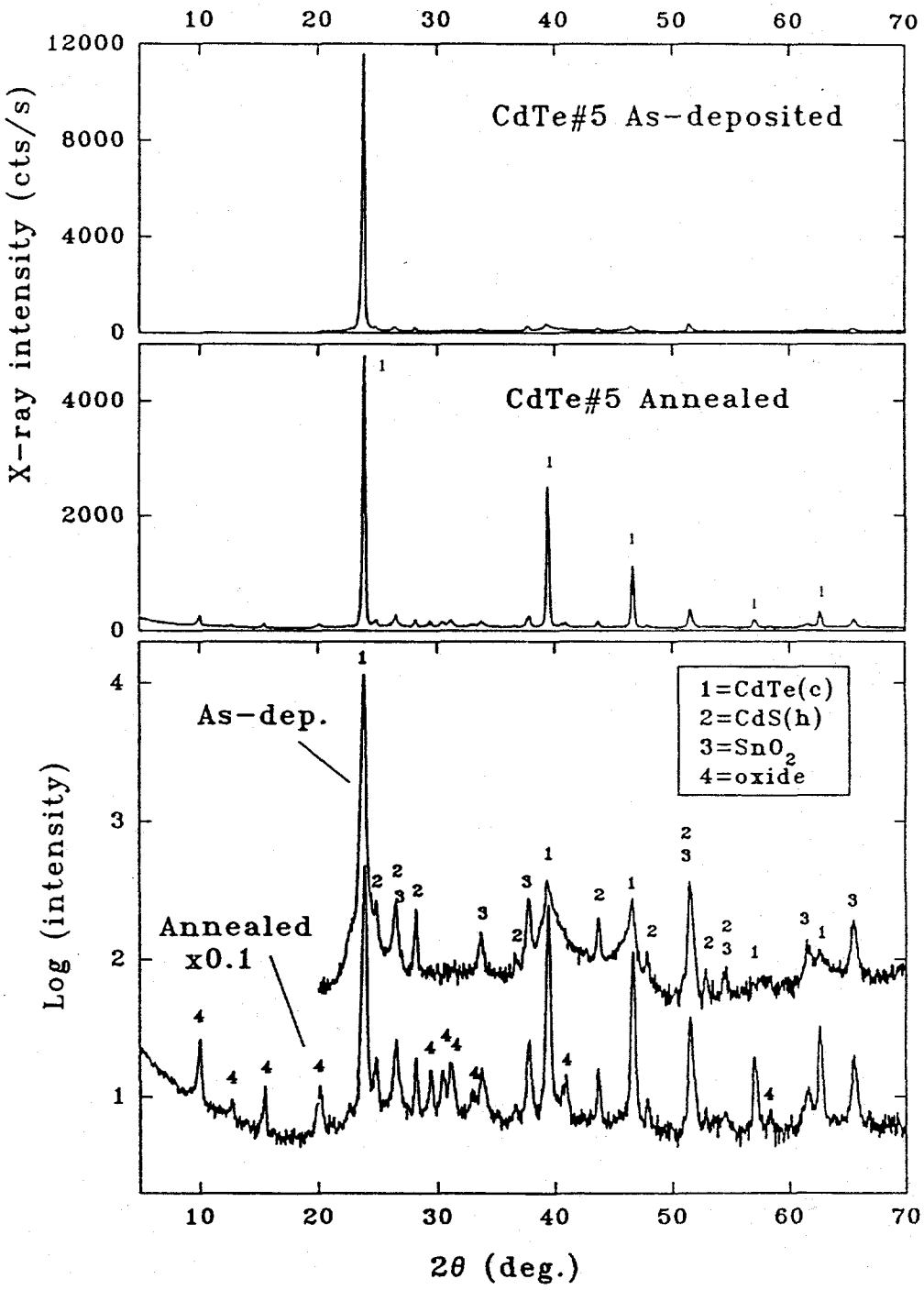

Figure 10. X-ray diffraction data for a CdTe film deposited onto CdS-coated, SnO_2-coated glass at CSM.

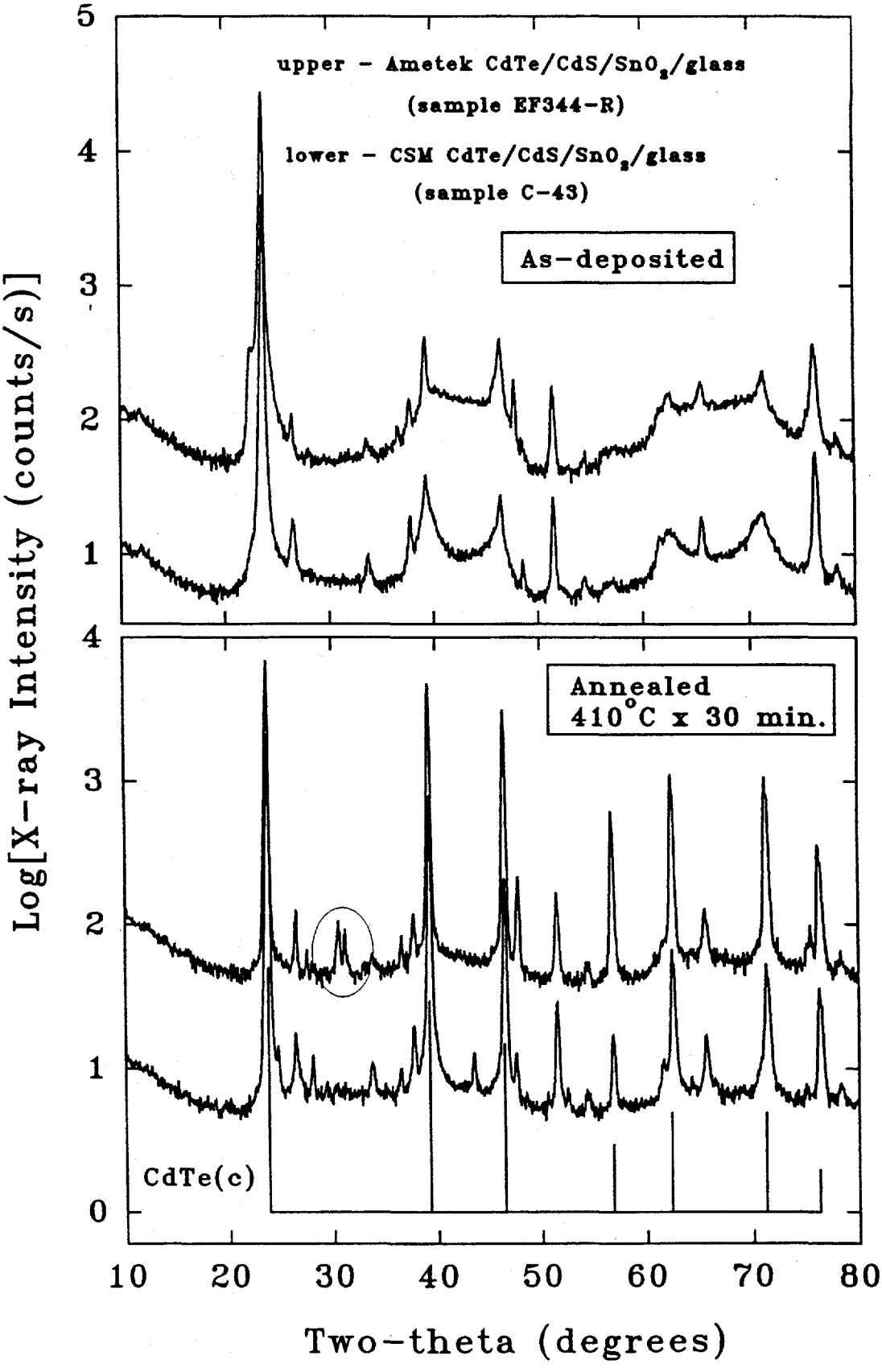

Figure 11. Comparison of XRD data for CdTe films made by Ametek and by CSM.

d) ZnTe Processing and Characterization

We have initiated exploratory research on an electrochemical method for depositing ZnTe, rather than relying on physical evaporation (the method used in the Ametek cell). P-type ZnTe is a superior back contact to the CdTe because of favorable alignment of the valence bands. This leads to a low barrier for hole collection at that junction.

Samples were grown under potentiostatic control in a solution of 1 M $ZnSO_4$, saturated with TeO_2. A variety of cathode potentials were explored. Analyses were conducted on the sample grown at -1.1 V_{sce}, for 4 hour. This condition yielded a deposition current density of about 300 $\mu A/cm^2$. The XRD results showed that, prior to annealing, there was some ZnTe with a large amount of elemental Te. During an annealing step (425 °C, in air) the Te in the electrodeposited layer nearly disappeared, and cubic ZnTe was formed.

We have performed a more detailed analysis of the requirements for this experiment. Those are summarized here:

The appropriate reactions for simultaneous deposition of Zn and Te are

$$(A)\ Zn \leftrightarrow Zn^{2+} + 2\ e^-$$
$$V_{Zn} = -0.76 + 0.0295 \log (a_{Zn2+} / a_{Zn}) \qquad (9)$$

$$(B)\ Te + 2H_2O \leftrightarrow HTeO_2^+ + 3H^+ + 4\ e^-$$
$$V_{Te} = 0.551 + 0.0148 \log (a_{HTeO2+} / a_{Te}) - 0.0443\ pH \qquad (10)$$

Here the potentials are expressed relative to the NHE standard reference. The activities of the elements in the compound are related, through the free enthalpy of formation of ZnTe:

$$a_{Zn}\, a_{Te} = \exp(G_{ZnTe} / RT) \qquad (11)$$

where G_{ZnTe} = -28.18 kcal/mole. As the potential of the cathode is changed, ZnTe has an existence range from the phase boundary at Zn/ZnTe (where the activity of Zn is 1), to the phase boundary at ZnTe/Te (where the activity of Zn is $a_{Zn} = \exp(G_{ZnTe} / RT)$, since $a_{Te} = 1$). This shift of a_{Zn} and a_{Te} causes the equilibrium potentials of Zn and Te to shift from those predicted by reactions (A) and (B), above. The compound formation shifts V_{Zn}^o from - 0.76 V, at the Zn/ZnTe phase boundary, to - 0.76 V - G_{ZnTe} / 2F = - 0.15 V, at the ZnTe/Te phase boundary, and V_{Te}^o from 0.551 V, at the ZnTe/Te phase boundary, to 0.551 V - G_{ZnTe} / 4F = 0.824 V, at the Zn/ZnTe phase boundary. At the phase boundary with Zn (the less noble component), $V_{Te}^o - V_{Zn}^o > 0$ while $G_{ZnTe} < 0$. This means $a_{Zn2+} >> a_{HTeO2+}$. So Zn is the potential determining component at that boundary. On the other hand, at the Te phase boundary, $V_{Te}^o - V_{Zn}^o > | G_{ZnTe} / 2F |$. So deposition of ZnTe is a "Class I" process, according to the scheme of Kröger [23], with Zn the potential determining species at this boundary also. Thus, the potential range over which ZnTe can be deposited is from - 0.76 + 0.0295 log (a_{Zn2+}) - Δ V, at the Zn/ZnTe boundary, to - 0.15 + 0.0295 log (a_{Zn2+}) - Δ V, at the ZnTe/Te boundary. Here, Δ V is the combination of the discharge

overpotential and the ohmic drop in the electrolyte.

Under the conditions of our test the concentrationof Zn was 1 M. This leads to a stability range for ZnTe, referenced to the SCE electrode, of - 0.361 V to -0.971 V. The potential of the cathode in the growth of the test sample was - 1.1 V, clearly outside of the acceptable range for ZnTe. There was, apparently, sufficient elemental deposition, however, to allow formation of the compound upon annealing. With our increased understanding of the energetics of this process, we should be able to make rapid progress on the electrodeposition of ZnTe. This bears much similarity to CdTe, in the electrochemistry of the system. However, there has been only one published account of efforts in this area[24] . In that study, ZnTe was grown by reacting a zinc-containing solution with a tellurium electrode. This method would not be suitable for our purposes.

As in CdTe electrodeposition, the rate of ZnTe compound formation is limited by the rate of deposition of Te. This, in turn, is limited by the low solubility of $HTeO_2^+$. For concentrations of TeO_2 above 0.001 M the solution is essentially saturated. This limitation to deposition rate could be partially overcome by the use of a sacrificial anode, as described by Gobrecht[25] to increase the concentration of $HTeO_2^+$ above the solubility limit.. This is the same approach followed by the Ametek process for CdTe. We expect it should be possible to employ a Te anode, as well as an inert (Pt) anode, biased in such a manner so as to maintain a current through the Te that is twice that through the Pt.

Figure 12 shows XRD data from one of our first attempts to produce ZnTe films by an electrochemical process. Note that a large amount of unreacted Te is present in the as-deposited film and that, after annealing, this phase practically disappears and cubic ZnTe is formed. Further work is needed to refine this process and to test the growth of ZnTe on the CdTe.

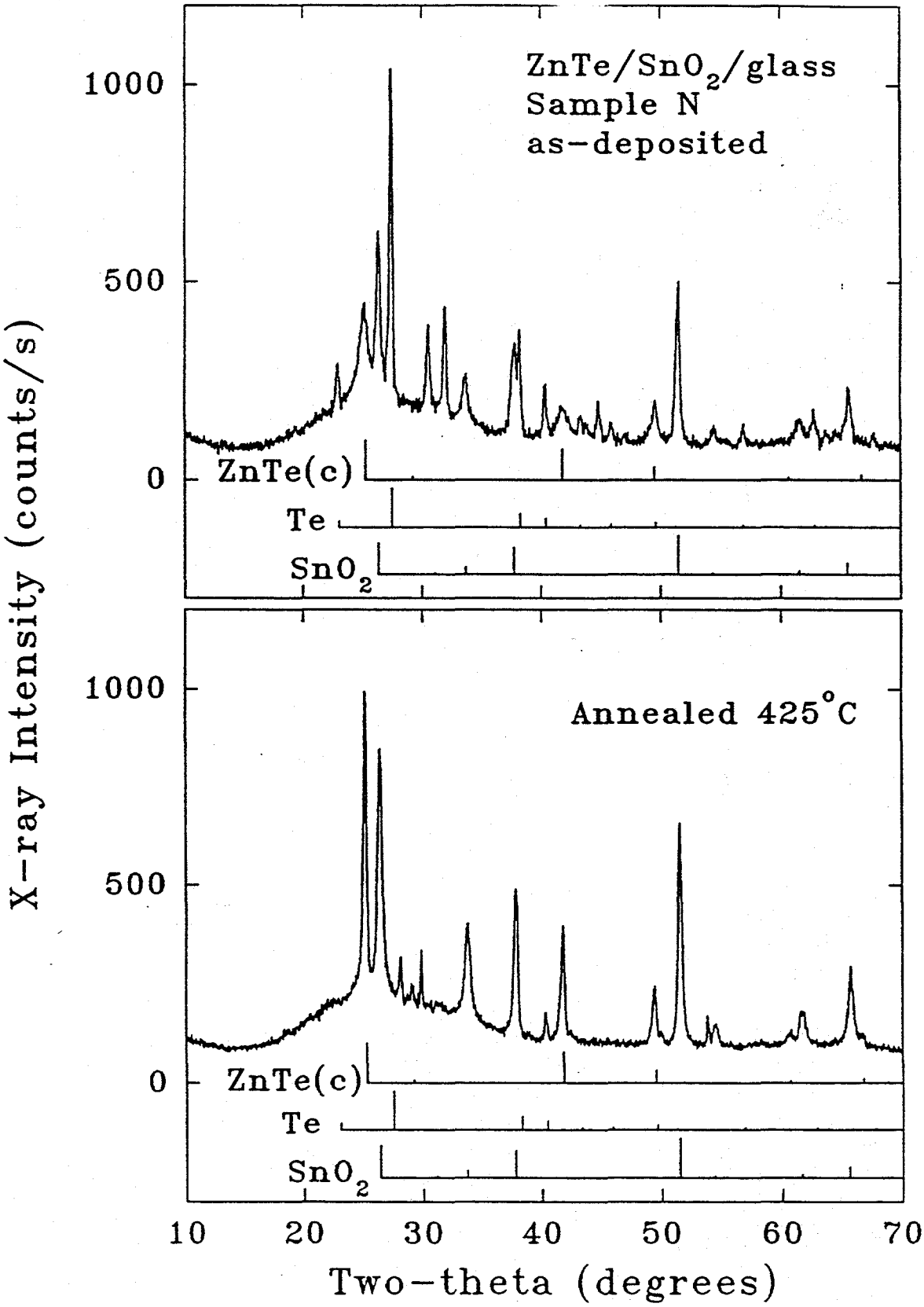

Figure 12. XRD data for electrochemically deposited ZnTe film.

e) Devices

Our major research effort to date has been spent in learning the electrochemical process, in understanding the role of each processing parameter, and in carrying out trouble-shooting as problems occur. Using a small, simple bath (1-2 liters), CdTe layers were deposited and dot-cells with an CdS/CdTe/Au structure have been made in order to estimate the quality of the CdTe layers.

In order to compare the performances of CdTe layers deposited at CSM with those of Ametek, a CdTe film was deposited on a CdS substrate made by Ametek. The sample was then annealed and etched before the Au deposition (sample C-34). A piece of CdTe sample from Ametek was also taken through the same post-deposition treatment (sample A-40). The only possible difference between the two samples developed in this fashion should be in the CdTe layer.

Table 1 shows the result of this experiment. The data indicate that a significant improvement

Table 1. Comparison of CdS/CdTe/Au dot cells made of CdTe layers deposited either by CSM (C-34) or by Ametek (A-40)

	V_{oc}, mV	J_{sc}, mA/cm^2	FF,%	η,%	R_s, Ωcm^2
C-34	576	16.4	44.7	4.25	1.8
A-40	734	21.3	56.3	8.82	0.92

in CdTe quality must be made in order to reproduce the Ametek results. Possible steps for improvement are as follows:

(i) Reduce the free carrier recombination both in the bulk and at the CdS/CdTe interface. The recombination at grain boundaries may be reduced by obtaining a columnar grain structure. Columnar growth occurs at an optimum deposition current density (0.45 mA/cm^2 reported by Ametek[20], 0.2-0.5 mA/cm^2 reported by Monosolar Inc.[21]). Recombination within the grains may be reduced by minimizing the incorporation of impurities and crystalline defects such as vacancies and interstitials of either Te or Cd. This can be done through enhancement of the cleanliness of the process and control of the deposition current ratio between the Te anode and the Cd anode (J_{Te}/J_{Cd}), respectively. A possible solution for reducing the interface recombination losses includes the reduction of crystalline defects through enhancing the cleanliness of the procedure and control of the annealing process. The $CdCl_2$ treatment before annealing is also reported to decrease the interface recombination.

(ii) Reduce the series resistance R_s. The higher R_s of C-34 may be due to the higher resistivity of the CdTe layer, since both C-34 and A-40 have the same nominal thickness of 2 μm and have undergone identical annealing and etching processes. Our higher resistivities may be a result of different compositions of the films. Some of Ametek's films were deposited at $J_{Te}/J_{Cd} = 3$, i.e., Cd-deficient conditions, whereas, C-34 was deposited at the stoichiometric condition (the current ratio of 2). Native defects such as cadmium vacancies are known to be electrically active as acceptors in CdTe. Another possibility is to reduce the incorporation of the compensating donor impurities. Optimization of the thickness of the CdTe layers is another step. Since the CdTe layers have high resisitivities (up to 10^7 Ωcm)[22], even a small variation of thickness such as 1000Å may result in a significant R_s increase.

(iii) Control the properties of the CdS layer. We need to optimize the thickness and the annealing process of CdS to ensure better optical transmission. Annealing may enhance the electrical conductivity and decrease recombination within the film by reducing the defect density.

The data from A-40 have some important implications. First, they will be used as a reference for the CdTe layers that will be produced at CSM. In other words, CdTe films comparable to those of Ametek should lead to cells with efficiencies close to 9%. Secondly, we believe that the post-deposition treatment at CSM is at a similar technical state to that of Ametek. Most of the Ametek cells had efficiencies near or slightly over 9% even though their cells had ZnTe/Ni contacts which are believed to have lower resistance than plain Au contacts. Therefore, we conclude that, at least for now, we should concentrate our effort on improving the CdTe deposition and annealing process.

So far, we have depended on materials characterization methods such as XRD and light current-voltage J-V measurements. We are initiating additional diagnostic tools such as electrical transport studies of the CdS/CdTe junction both in dark and light conditions, spectral response at different bias conditions, and electron beam induced current measurements to better characterize the materials and the cells.

Recent progress of this project has been at an accelerated pace, as our understanding and experience have accumulated. Figure 13 shows cell efficiencies vs the elapsed time during the past few months. We will switch to a larger bath with a filtration system for the CdTe deposition in the near future. Based on the fact that we have pinned down most of the processing problems, we expect that, within a few months, we will produce CdTe films as a routine procedure. With additions to our work force and more working space, we believe that we will soon reproduce the Ametek cell efficiency (11% - 12% for 1 cm^2 cells) through systematic studies. New investigations for improved efficiencies and processing techniques will become of highest priority at that point.

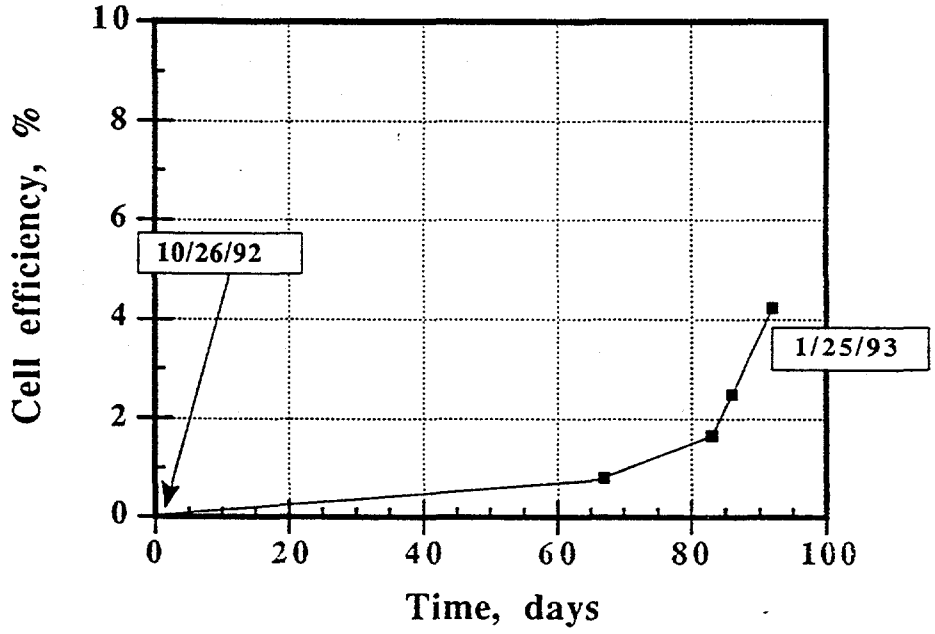

Figure 13. Recent CSM dot-cell efficiencies versus time. The cell structure is glass/SnO_2/CdS/CdTe/Au and the size is 0.03 cm^2.

f) Analytical Facilities

As implied throughout this report, a number of analytical facilities at CSM have been employed for the characterization of both materials and complete devices. Additional facilities are currently being developed or improved.

The materials-characterization facilities include XRD, Raman Spectroscopy, and SAXS systems. Representative data from each of these was included in the preceeding pages. To our knowledge, the SAXS data for CdS represent the first such results on this material. We have also installed and made routine use of a scanning electron microscope (with EDX), an alpha-step profilimeter, and a four-point probe, all acquired from Ametek.

For the characterization of complete cells, our primary measurement to date has been of standard I-V curves under a broad-band light source. This apparatus is currently being upgraded with an improved software package for data storage, curve-fitting, and the determination of key cell parameters. Equipment for C-V determinations has also been installed but is not yet in routine use. Both of these facilities were acquired from Ametek.

Other instrumentation which will be set up, tested, and utilized in the near future includes apparatus to measure spectral response and a solar simulator. We will also be designing further upgrades to the I-V apparatus and to the four-point probe to allow measurements to be made as a function of temperature.

7. Summary and Plans

We have made substantial progress on most of the "Phase I" tasks as listed in Section 5 of this report. Regarding film growth techniques, the dip-coating process is established as an alternative to spray pyrolysis for the deposition of the n-type CdS layer. In the case of the CdTe layer, we have not yet investigated the effects of photoenhancement on the electrochemical process. However, we have gained a significant understanding of the basic electrochemistry of this material and have established a foundation for photoenhancement studies in Phase 2 of the project. We have demonstrated that it is possible to use an electrochemical process to deposit thin films of ZnTe. This work will be pursued in Phase 2. Finally, although rapid thermal processing has not yet been investigated, we are in a position to do so in Phase 2 now that the basic processes for each of the layers have been defined.

With regard to device fabrication, dot cells of regularly increasing efficiency are now being fabricated in the geometry glass/SnO_2/CdS/CdTe/Au. We have also developed a photoresist technique for blocking pinholes in the CdTe layer and have measured uniform dot-cell efficiencies over large areas using this process. Thus, we expect to demonstrate high-efficiency 1 cm^2 cells in the near future.

Finally, the Phase I tasks of establishing facilities for materials analysis and for device characterization have been accomplished as described in the report.

In view of the results of Phase 1 of this project, a revised list of Phase 2 and Phase 3 tasks and goals is given on the following pages.

Phase Two Tasks

Task five (high quality film growth techniqes)

1. Optimize the procedures of preference for the fabrication of TCOs, CdS, CdTe, ZnTe, and contact layers, including studies of the effects of photoenhancement on the electrochemical deposition of CdTe with respect to grain size, grain boundary passivation, and other characteristics of the product.

2. Conduct experiments with rapid thermal processing.

3. Combine the selected processes for individual layers into a single procedure for the fabrication of entire cells.

4. Determine the most effective processing steps for the mitigation of electronic traps.

5. Publish results in open literature.

Task six (device fabrication)

1. Demonstrate a 1 cm^2 cell which has been made using the preferred procedures.

2. Demonstrate a 12%, 1 cm^2 cell.

3. Develop a manufacturable module which incorporates these cells, including appropriate encapsulation.

4. Develop the preliminary design of a large-scale process suitable for the production of CdTe modules.

Task seven (material analysis and device characterization)

1. Demonstrate the use of STM or other techniques to characterize the electrical potential distribution near grain boundaries and interfaces as it relates to the depression of V_{oc}.

Phase Three Tasks

Task eight (high quality film growth techniques)

1. Optimize the procedures of preference for the fabrication of CdS, CdTe, and ZnTe layers.

2. Combine the selected processes for individual layers into a single procedure for the fabrication of entire cells.

3. Determine the most effective processing steps for the mitigation of electronic traps.

4. Publish results in open literature.

Task nine (device fabrication)

1. Demonstrate a 13%, 1 cm^2 cell.

2. Develop a manufacturable module which incorporates these cells, including appropriate encapsulation.

8. References

1. P.V. Meyers, Solar Cells 24, 35 (1988).

2. J.M. Digueroa, F. Sanchez-Sinencio, J.G. Mendoza-Alvarez, D. Zelaya, C. Vazquez-Lopez, and J.S. Helman, J. Appl. Phys. 60, 452 (1986).

3. Y. Qu, T.A. Gessert, K. Ramanathan, R.G. Dhere, R. Noufi, and T.J. Coutts, Proceedings 39th AVS National Symposium, in press.

4. Inderjeet Kaur, D.K. Pandya, and K.L. Chopra, J. Electrochem. Soc. 127, 943 (1980).

5. N.R. Pavaskar, C.A. Menezes, and A.P.B. Sinha, J. Electrochem. Soc. 124, 743 (1977).

6. A. Mondal, T.K. Chaudhuri, and P. Pramanik, Solar energy Materials 7, 431 (1983).

7. T.L. Chu, Shirley A. Chu, N. Schultz, C. Wang, and C.Q. Wu, J. Electrochem. Soc. 139, 2443 (1992).

8. D.S. Chuu, C.M. Dai, W.F. Hsieh, and C.T. Tsai, J. Appl. Phys. 69, 8402 (1991).

9. D. Kim, A.L. Fahrenbruch, A. Lopez-Otero, and R.H. Bube, Proc. Materials Research Society, 1992, Spring Meeting, Symposium E. San Francisco, 1992.

10. M.P.R. Panicker, M. Knaster, and F.A. Kroger, J. Electrochem. Soc.: Electrochemical Sicence and Technology 125, 566 (1977); F.A. Kroger, J. Electrochem. Soc.: Solid-State Science and Technology 125, 1028 (1978).

11. Ametek notebook (1983).

12. M.P.R. Panicker, M. Knaster, and F.A. Kroger, J. Electrochem. Soc.: Electrochemical Sicence and Technology 125 566 (1977); F.A. Kroger, J. Electrochem. Soc.: Solid-State Science and Technology 125 1028 (1978); S. Bonilla and E.A. Dalchiele, Thin solid Films 204 394 (1991); S.K. Das and G.C. Morris, J. Appl. Phys., 72 4940 (1992); M. Takahashi, K. Uosaki, and H. Kita, J. Appl. Phys. 58 4292 (1985); R.L. Rod, R. Bunshah, O. Stafsudd, B.M. Basol, P. Nath, Final report for DOE contract DE-AC04-79ET23008 (1980).

13. S.M. Babu, R. Dhanasekaran, and P. Ramasamy, Thin Solid films 202 67 (1991).

14. R.L. Rod, R. Bunshah, O. Stafsudd, B.M. Basol, P. Nath, Final report for DOE contract DE-AC04-79ET23008 (1980).

15. R.B. Gore, R.K. Pandey, and S.K. Kulkarni, J. Appl. Phys. 65 1693 (1989).

16. M.P.R. Panicker, M. Knaster, and F.A. Kroger, J. Electrochem. Soc.: Electrochemical Science and Technology, 125 566 (1977); B.M. Basol, J. Appl. Phys. 55 601 (1984).

17. A. Compaan, R.G. Bohn, A. Bhat, C. Tabory, M. Shao, Y. Li, M.E. Savage, and L. Tsien, AIP Conf. Proc. 268 PV AR&D Project, Denver, 255 (1992).

18. A. Rohatgi, H.C. Chou, A. Bhat, and R. Sudharsanan, AIP Conf. Proc. 268 PV AR&D Project, Denver, 243 (1992).

19. J.P. Haering, J.G. Werthen, R.H. Bube, L. Gulbrandsen, W. Jansen, and P. Luscher, J. Vac. Sci. Technol. A1 1469 (1983).

20. Obtained from Ametek's deposition log sheets.

21. R.L. Rod, R. Bunshah, O. Stafsudd, B.M. Basol, P. Nath, Final report for DOE contract DE-AC04-79ET23008 (1980).

22. P.V. Meyers, Final report for SERI subcontract ZL-7-06031-2

23. F.A. Kröger, J. Electrochemical Soc. 125, 2028 (1978).

24. H.J. Gerritsen, J. Electrochemical Soc. 131, 136 (1984).

25. H. Gobrecht, H.D. Liess, and A. Tausend, Ber. Bunsenges. Phys. Chem. 67, 930 (1973).

9. Appendices

a) Personnel

Thirteen individuals have contributed to this work since its inception in March, 1992. Their names, titles, and representative responsibilities are summarized below. Those who have been involved during just a portion of the project period are noted.

Permanent Faculty

1. Thomas E. Furtak, Professor of Physics: electrochemistry, optical properties

2. John U. Trefny, Professor of Physics: project coordinator

3. Noboru Wada, Associate Professor of Physics: Raman spectroscopy

4. Don L. Williamson, Professor of Physics: XRD, SAXS

Research Associate; Temporary Faculty

5. Donghwan Kim, Research Associate: materials processing and characterization (since October 26, 1992).

6. Nashwa Shalaan, Visiting Professor: sample characterization (September - November, 1992).

7. Nic Dalacu, Consultant: electrochemical processing (approximately 30 days total between March and September, 1992).

Students

8. Stefan Araz, Undergraduate: XRD (June-December, 1992)

9. Dahong Du, Graduate Research Assistant: CdS processing

10. Scott Pozder, Graduate Research Assistant: electrochemical processing

11. Yi Qu, Graduate Research Assistant: TCO coatings

12. Jason Selby, Graduate Research Assistant: four-point probe (January, 1993 - present)

13. Yuming Zhu, Graduate Research Assistant: I-V measurements (January, 1993 - present)

b) Laboratory Improvements

Since the inception of this project, Colorado School of Mines has spent or committed more than $100,000 for laboratory improvements and equipment upgrades. The majority of these funds has been used to provide the processing laboratory with modern, filtered fume hoods and other hardware related to the safety of staff members and students working on the project. One eight-foot hood was installed in the summer of 1992; a second will be completed this spring.

Additional investments have been made in a de-ionized water system and in the servicing and rehabilitation of the scanning electron microscope received from Ametek. A great deal of time and study has been devoted to safety issues in general. Routine testing of personnel as well as air and wipe tests in the laboratory have been established toward this end.

c) Publications

1. J.U. Trefny, Polycrystalline CdTe Solar Cells for Large-Scale Space Applications, Proceedings Space '92, in press.

2. Y. Qu, T.A. Gessert, K. Ramanathan, R.G. Dhere, R. Noufi, and T.J. Coutts, Electrical and Optical Properties of Ion-Beam Sputtered Al-Doped ZnO Films as a Function of Film Thickness, Proceedings 39th AVS National Symposium, in press.

Document Control Page	1. NREL Report No. NREL/TP-451-5652	2. NTIS Accession No. DE93018201	3. Recipient's Accession No.

4. Title and Subtitle
Polycrystalline Thin-Film Cadmium Telluride Solar Cells Fabricated by Electrodeposition

5. Publication Date
August 1993

6.

7. Author(s)
J.U. Trefny, T.E. Furtak, N. Wada, D.L. Williamson, D. Kim

8. Performing Organization Rept. No.

9. Performing Organization Name and Address

Colorado School of Mines
Department of Physics
Golden, Colorado 80401

10. Project/Task/Work Unit No.
PV331101

11. Contract (C) or Grant (G) No.
(C) XG-2-11036-4
(G)

12. Sponsoring Organization Name and Address
National Renewable Energy Laboratory
1617 Cole Blvd.
Golden, CO 80401-3393

13. Type of Report & Period Covered
Technical Report
20 March 1992 - 19 March 1993

14.

15. Supplementary Notes
NREL technical monitor: B. von Roedern

16. Abstract (Limit: 200 words)

This report describes progress during the first year of a 3-year program at Colorado School of Mines, based upon earlier studies performed by Ametek Corporation, to develop specific layers of the Ametek n-i-p structure as well as additional studies of several transparent conducting oxides. Thin films of ZnO and ZnO:Al were deposited under various conditions. For the n-layer of the Ametek structure, a dip-coating method was developed for the deposition of CdS films. We also present data on the characterization of these films by X-ray diffraction, Raman spectroscopy, scanning tunneling microscopy, small-angle X-ray scattering, and other techniques. We made progress in the electrodeposition of the CdTe i-layer of the Ametek structure. We developed appropriate electrochemical baths and are beginning to understand the role of the many experimental parameters that must be controlled to obtain high-quality films of this material. We explored the possibility of using an electrochemical process for fabricating the ZnTe p-layer. Some preliminary success was achieved, and this step will be pursued in the next phase. Finally, we fabricated a number of "dot" solar cells with the structure glass/SnO_2/CdS/CdTe/Au. Several cells with efficiencies in the range of 5%–6% were obtained, and we are confident, given recent progress, that cells with efficiencies in excess of 10% will be achieved in the near future.

17. Document Analysis
a. Descriptors
polycrystalline ; thin film ; cadmium telluride ; electrodeposition ; photovoltaics ; solar cells

b. Identifiers/Open-Ended Terms

c. UC Categories
273

18. Availability Statement
National Technical Information Service
U.S. Department of Commerce
5285 Port Royal Road
Springfield, VA 22161

19. No. of Pages
42

20. Price
A03

Form No. 0069E (6-30-87)